Bioorganic & Medicinal Chemistry 19 (2011) 5967–5974

Contents lists available at SciVerse ScienceDirect

Bioorganic & Medicinal Chemistry

journal homepage: www.elsevier.com/locate/bmc

Solid-state NMR analysis of interaction sites of curcumin and 42-residue amyloid β-protein fibrils

Yuichi Masuda [a,b,*], Masashi Fukuchi [b], Tatsuya Yatagawa [b], Masato Tada [b], Kazuyuki Takeda [b], Kazuhiro Irie [c], Ken-ichi Akagi [d], Youko Monobe [d], Takayoshi Imazawa [d], K. Takegoshi [b]

[a] Graduate School of Pharmaceutical Sciences, Tohoku University, 6-3 Aza-Aoba, Aramaki, Aoba-ku, Sendai 980-8578, Japan
[b] Department of Chemistry, Graduate School of Science, Kyoto University, Kitashirakawa Oiwake-cho, Sakyo-ku, Kyoto 606-8502, Japan
[c] Division of Food Science and Biotechnology, Graduate School of Agriculture, Kitashirakawa Oiwake-cho, Sakyo-ku, Kyoto 606-8502, Japan
[d] Laboratory of Common Apparatus, Division of Biomedical Research, National Institute of Biomedical Innovation, 7-6-8 Saito-Asagi, Ibaraki, Osaka 567-0085, Japan

ARTICLE INFO

Article history:
Received 12 July 2011
Revised 24 August 2011
Accepted 24 August 2011
Available online 27 August 2011

Keywords:
Amyloid β-protein
Curcumin
Solid-state NMR
Covariance
β-Sheet

ABSTRACT

Aggregation of 42-residue amyloid β-protein (Aβ42) plays a pivotal role in the etiology of Alzheimer's disease (AD). Curcumin, the yellow pigment in the rhizome of turmeric, attracts considerable attention as a food component potentially preventing the pathogenesis of AD. This is because curcumin not only inhibits the aggregation of Aβ42 but also binds to its aggregates (fibrils), resulting in disaggregation. However, the mechanism of interaction between curcumin and the Aβ42 fibrils remains unclear. In this study, we analyzed the binding mode of curcumin to the Aβ42 fibrils by solid-state NMR using dipolar-assisted rotational resonance (DARR). To improve the quality of 2D spectra, 2D DARR data were processed with the covariance NMR method, which enabled us to detect weak cross peaks between carbons of curcumin and those of the Aβ42 fibrils. The observed ^{13}C–^{13}C cross peaks indicated that curcumin interacts with the 12th and 17–21st residues included in the β-sheet structure in the Aβ42 fibrils. Interestingly, aromatic carbons adjacent to the methoxy and/or hydroxy groups of curcumin showed clear cross peaks with the Aβ42 fibrils. This suggested that these functional groups of curcumin play an important role in its interaction with the Aβ42 fibrils.

1. Introduction

Alzheimer's disease (AD) is generally characterized by the formation of senile plaques in the brain cortex.[1] The major components of the senile plaques are aggregates of 40- and 42-residue amyloid β-protein (Aβ40 and Aβ42, respectively)[2,3] derived from proteolytic cleavage of amyloid precursor protein (APP)[4] by β- and γ-secretases.[5] Aggregation of Aβ causes neuronal death, which is associated with oxidative stress, mitochondrial dysfunction, disruption of membrane integrity, abnormal calcium homeostasis, and induction of the apoptotic pathways.[6,7] Aβ42 is believed to play a crucial role in the pathogenesis of AD because it is predominant in the senile plaques of AD patients[8] and significantly aggregative and neurotoxic.[9,10]

The structure of the Aβ aggregates (fibrils) has been studied extensively to reveal the aggregation mechanism and develop new agents that inhibit aggregation. So far, it has been shown that the Aβ fibrils are 7–12 nm in diameter and composed of several protofilaments, which are 3–6 nm in diameter.[11–13] The Aβ fibrils have a cross-β structure, in which β-strands lie perpendicular to the fiber axis and form intermolecular parallel β-sheets in both Aβ40 and Aβ42.[12–15] Numerous studies proposed models of tertiary structures of the Aβ fibrils by systematic replacement with proline,[16] solution NMR in combination with hydrogen/deuterium exchange,[17–20] and solid-state NMR.[21,22] We also proposed a structural model of the Aβ42 fibrils related to their neurotoxicity by systematic proline replacement and solid-state NMR.[23–27] The N-terminus is believed to be unstructured in both Aβ40 and Aβ42 fibrils. All the structural models of Aβ42 adopt β-sheets in the C-terminus as opposed to most models of Aβ40. In the central region, the intermolecular parallel β-sheets exist separated by a turn or bend structure, whose position slightly differs among the models. The neurotoxicity of Aβ could be reportedly ascribed to soluble Aβ aggregates (oligomers),[28,29] whose structure has become a subject of recent research.[30,31]

Small molecules that specifically and efficiently inhibit the Aβ aggregation could be therapeutic agents for AD. Congo red[32] and β-sheet breaker peptide[33] are well-known inhibitors of Aβ aggregation; however, these artificial compounds require further efforts for evaluating their safety and modifying their structures to render them suitable for human therapeutics. Recent studies have shown that polyphenolic compounds from food products, such as green tea and red wine, have potent anti-aggregating activity.[34–37]

* Corresponding author. Tel.: +81 22 795 6868; fax: +81 22 795 6864.
E-mail address: masuda@mail.pharm.tohoku.ac.jp (Y. Masuda).

0968-0896/$ - see front matter © 2011 Elsevier Ltd. All rights reserved.
doi:10.1016/j.bmc.2011.08.052

Among these polyphenols, curcumin (diferuloylmethane), the yellow pigment in the rhizome of turmeric (*Curcuma longa*), attracts considerable attention as a food component preventing the pathogenesis of AD.[38] Although the difference of life expectancies should be considered, epidemiological studies reported that India, where curcumin consumption is widespread, has a lower incidence of AD than the United States.[39] In vitro studies have shown that curcumin not only inhibits the Aβ aggregation but also disaggregates the Aβ fibrils.[40,41] In vivo studies using AD transgenic mice have shown that chronic dietary curcumin lowered Aβ deposition in the brain,[42] and intravenously injected curcumin crossed the blood-brain barrier and bound to the amyloid plaques.[41,43] Interestingly, systemic treatment of mice with curcumin reduced new amyloid accumulation as well as previously deposited amyloid plaques.[43] This can be attributed to the potency of curcumin to disaggregate the Aβ fibrils and inhibit Aβ aggregation as previously described in vitro.[40,41] Because curcumin shows a wide range of properties, such as anti-inflammation, anti-oxidation, metal chelation, and maintenance of protein homeostasis,[38,42,44–48] the possibility that some other actions contribute to the clearance of amyloid deposits in vivo cannot be neglected. In any case, the binding of curcumin to the amyloid deposits could be closely related to their reduction.

Elucidating the interaction sites of curcumin and the Aβ42 fibrils and important structural features of curcumin contributing to its potency as an inhibitor is essential for understanding the mechanism of interaction and developing new medicinal leads. However, no substantial experimental data directly showing the binding mode of curcumin to the Aβ42 fibrils has been recorded except for some structure–activity studies.[44,49] Solid-state NMR is an effective tool to analyze the interaction between solid (amyloid fibrils) and solute (curcumin dissolved in water). In this study, we analyzed the binding mode of curcumin to the Aβ42 fibrils by solid-state NMR. The application of covariance processing[50–53] to improve the 2D spectra quality is also discussed.

2. Results and discussion

2.1. Syntheses of Aβ42 and curcumin selectively labeled with ^{13}C

To analyze the intermolecular dipole–dipole interactions between the Aβ42 fibrils and curcumin by solid-state NMR, we selectively labeled the Aβ42 peptide and curcumin with ^{13}C. As mentioned in Section 1, Aβ forms intermolecular β-sheets to aggregate.[12–15] Most of the aggregation inhibitors, including curcumin, possess planar structures,[32,34–37] which could be easily intercalated between β-sheets. Moreover, curcumin does not bind to the Aβ monomers, but to the protofibrils and the fibrils, both of which are rich in β-sheets.[41] On the basis of these data, we expected curcumin to interact with the β-sheet region of Aβ42. Although various different structural models of the Aβ42 fibrils have been proposed,[16–27] it is widely accepted that the amino acid residues at positions 17–21 form intermolecular parallel β-sheets and those at the N-terminus form a random coil structure. In addition, F19 and F20 in the Aβ42 fibrils could form intermolecular π–π stacking interactions, which can be inhibited by the aromatic rings of curcumin.[34,54] Therefore, we synthesized Aβ42 labeled at positions 17–21 with ^{13}C (Fig. 1A), along with Aβ42 labeled at the N-terminus with ^{13}C for comparison (Fig. 1B). Nitrogen atoms were labeled with ^{15}N to avoid the influence of ^{14}N quadrupole interaction on ^{13}C.[55,56] To avoid signal overlap, only aromatic carbons were labeled in curcumin (Fig. 1C) and only non-aromatic carbons were labeled in Aβ42 (Fig. 1A and B).

The ^{13}C-labeled peptides and curcumin were chemically synthesized. In short, the Aβ42 peptides can be synthesized in high yields using HATU[57] as an effective coupling activator for fluorenylmethoxycarbonyl (Fmoc) chemistry as previously reported.[58] Because Aβ42 easily aggregates under acidic and neutral conditions, purification by HPLC was performed under alkaline conditions.[59] Curcumin labeled at the aromatic carbons was synthesized from acetylacetone and ^{13}C-labeled vanillin using the method developed by Pabon (Scheme S1).[60]

A. Aβ42 labeled at positions 17—21:

DAEFRHDSGYEVHHQK**LVFFA**EDVGSNKGAIIGLMVGGVVIA
1 17 21 42

B. Aβ42 labeled at the N-terminus:

D**A**E**F**RHDS**G**YE**V**HHQKLVFFAEDVGSNKGAIIGLMVGGVVIA
2 4 9 12

C. Curcumin labeled at the aromatic carbons:

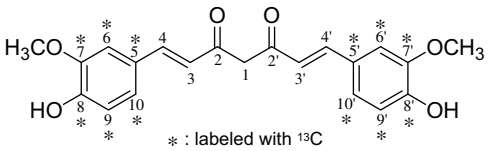

Figure 1. Selective labeling of Aβ42 and curcumin with ^{13}C and ^{15}N. Labeling scheme in the Aβ42 sequence: red letter, uniformly labeled with ^{13}C and ^{15}N; blue letter, only C_β is labeled with ^{13}C. Curcumin was labeled at its aromatic carbons with ^{13}C.

2.2. Preparation of ^{13}C-labeled Aβ42 fibrils mixed with ^{13}C-labeled curcumin

Because this study focuses on the binding mode of curcumin to the Aβ42 fibrils, ^{13}C-labeled curcumin was added after fibrillation of ^{13}C-labeled Aβ42 (Fig. S1). Incubation of ^{13}C-labeled Aβ42 (10 μM) in phosphate buffered saline (PBS) at 37 °C for 48 h gave white fibrils. To the fibril suspension, a five-fold excess of ^{13}C-labeled curcumin (50 μM) was added. Relatively higher concentration of curcumin was employed to accurately detect intermolecular interactions. Because the Aβ42 fibrils were stained orange immediately after adding curcumin, the mixture was incubated for only 1 h. After centrifugation, the orange-colored fibrils stained with curcumin were washed with distilled water, dried in vacuo, and used for solid-state NMR experiments.

The morphology of the Aβ42 fibrils stained with curcumin was examined by transmission electron microscopy (TEM) (Fig. S2). The morphology of the Aβ42 fibrils with curcumin was similar to that without curcumin. Because the co-incubation time with curcumin was only 1 h, the fibril structures could not have changed significantly before and after the addition of curcumin. Ono et al. previously suggested that curcumin rapidly destabilizes the Aβ fibrils because adding curcumin to the Aβ fibrils showed significant decrease in the fluorescent intensity within one hour in their thioflavin T (ThT) assay.[40] However, Hudson et al. recently reported that curcumin significantly biases the ThT fluorescence because of direct interaction of curcumin with ThT and/or competitive binding of curcumin with ThT to the fibrils.[61] For this reason, one cannot convincingly ascribe the decrease in the ThT fluorescence by curcumin to destabilization of the Aβ42 fibrils. On the other hand, other TEM studies observed destabilization of amyloid fibrils 3–7 day after adding curcumin to the amyloid fibrils.[41,62] Moreover, Yang et al. demonstrated dissolution of the Aβ42 fibrils after 3-day co-incubation with curcumin using sandwich ELISA.[41] Altogether, destabilization of amyloid fibrils by curcumin is likely to occur after long-time co-incubation.

2.3. Solid-state NMR experiments

2.3.1. ^{13}C 1D spectra

Figure 2 shows ^{13}C 1D spectra of the ^{13}C-labeled Aβ42 fibrils mixed with ^{13}C-labeled curcumin. Signals around 100–150 ppm indicate binding of ^{13}C-labeled curcumin to the Aβ42 fibrils. Cross polarization (CP) efficiency did not significantly affect the signal intensity ratio of curcumin to the Aβ42 fibrils among the contact-time of 0.5–2 ms. Since we used ramped-amplitude cross polarization (RAMP-CP),[63] the CP efficiency could not be very different among carbons with different numbers of attached protons. Therefore, we estimated the ratio of bound curcumin to Aβ peptide, measured from the signal intensity, to be ca. 1:4, assuming that the CP efficiency is almost same for all carbons. This implies that one curcumin molecule interacts with more than one Aβ molecule. Considering the previous report that curcumin does not bind to monomeric Aβ, but to the protofibrils and the fibrils,[41] the curcumin molecules are expected to exist across or between the Aβ molecules in the fibrils.

2.3.2. Application of covariance processing to 2D NMR data

For structural analysis, we used dipolar-assisted rotational resonance (DARR,[64,65] also known as RAD[66]), which realizes 2D distance-related solid-state NMR spectroscopy. In the 2D Fourier transform (FT) DARR spectra (Fig. S3), it was difficult to analyze weak intermolecular cross peaks buried in noise, which was mainly comprised of t_1 noise. To obtain a better representation of the 2D spectrum, we applied covariance data processing.[50–53] Covariance matrix C is obtained from $C = (F^{T} \cdot F)^{1/2}$, where F is the 2D NMR data processed by FT along the t_2 dimension only, F^{T} is its transpose, and superscript 1/2 designates the square root of the entire matrix. On the processed spectrum, the covariance values are shown as the intensity of cross peaks between ^{13}C spins causing magnetization transfer. Covariance processing of the 2D NMR data has proven to be useful for improving the signal to noise ratio (SNR), reduction of measurement time, and symmetrization of a 2D spectrum.[50,51,53] Covariance processing is reportedly beneficial for the ^{13}C–^{13}C correlation spectra of solid biomolecules such as microcrystalline proteins and amyloid fibrils.[67,68]

The spectra shown in Figure 3 were obtained by covariance-processing of the 2D DARR data (2D FID data is the same as those in Fig. S3). Intramolecular cross peaks in the covariance-processed spectra (Fig. 3) were observed at the same positions as those in the FT spectra (Fig. S3) with a better SNR. Moreover, intermolecular cross peaks appeared between the Aβ42 fibrils and curcumin (blue squares in Fig. 3C and D). Tekely and Brüschweiler recently reported that the improvement of SNR by covariance processing enabled them to detect some weak cross peaks that were not observed in the 2D FT spectra.[67] They also reported that covariance processing is not susceptible to artifacts under their experimental conditions when the number of t_1 points is sufficiently large (more than 128 points in their experiments).[67] To confirm that the intermolecular cross peaks observed in our experiments (blue squares in Fig. 3C and D) are not artifacts, we evaluated the mixing time dependence of the cross peaks. In the covariance-processed spectra at a mixing time of 50 ms (Fig. 3A and B), the intermolecular cross peaks were significantly weak for detection. One-dimensional cross section spectra at the ^{13}C chemical shift of positions 7 (7') and 8 (8') of curcumin (148.6 ppm, red line in Fig. 3) demonstrates that the cross peaks apparently got larger in proportion to the mixing time (Fig. 4). Our simulation study using two spin systems also confirmed the correlation between the mixing time and the cross-peak intensity in the covariance-processed spectra (Figs. S8–S10). These data strongly support the fact that the observed intermolecular cross peaks (blue squares inFig. 3C and D) arise from the ^{13}C–^{13}C dipolar interaction reintroduced by DARR during the mixing time. In 2D DARR spectra at the mixing time of 50 ms, the cross-peaks of carbon atoms indicate that their distance is 1.5–3.0 Å. On the other hand, when the mixing time is 500 ms, cross-peaks between carbons 5–6 Å apart are also observed. Thus, the observed intermolecular cross peak between carbons of curcumin and the Aβ42 fibrils suggest that their distance is 4–6 Å.

2.3.3. Investigation of interaction sites between curcumin and Aβ42 fibrils

In the covariance-processed 2D DARR spectrum at a mixing time of 500 ms (Figs. 4C and 5A), we observed several cross peaks between the carbons of curcumin and the residues at positions 17–21 of the Aβ42 fibrils. This suggests that curcumin interacts with theses residues which are included in the central β-sheet region of the Aβ42 fibrils. Curcumin had cross peaks with the methyl, methylene, methine, and carbonyl carbons of all the residues. This indicates that the binding of curcumin is not specific to a particular residue in the β-sheet region of the Aβ42 fibrils. Cole's group also suggested that the binding of curcumin to Aβ does not depend on the primary sequence but on the fibril-related conformation such as β-sheet because curcumin binds to the protofibrils and the fibrils made of short Aβ fragments, such as $A\beta_{1-28}$, $A\beta_{12-28}$, and $A\beta_{25-35}$.[41] This speculation is supported by the finding that curcumin is able to interact with other β-sheet-rich amyloid proteins such as α-synuclein and prion protein.[69,70]

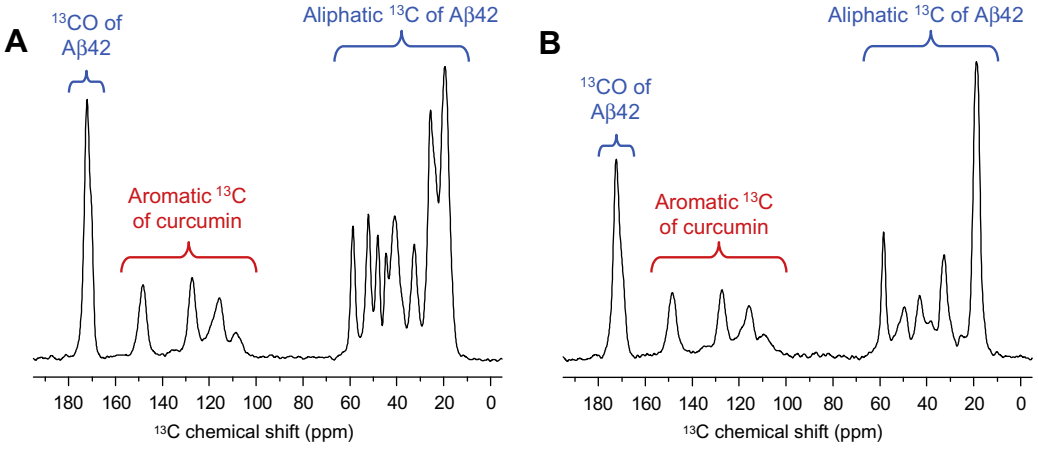

Figure 2. 1D ^{13}C CP/MAS spectra of Aβ42 fibrils labeled at positions 17–21 mixed with curcumin labeled at the aromatic carbons (**A**) and Aβ42 fibrils labeled at the N-terminus mixed with curcumin labeled at the aromatic carbons (**B**).

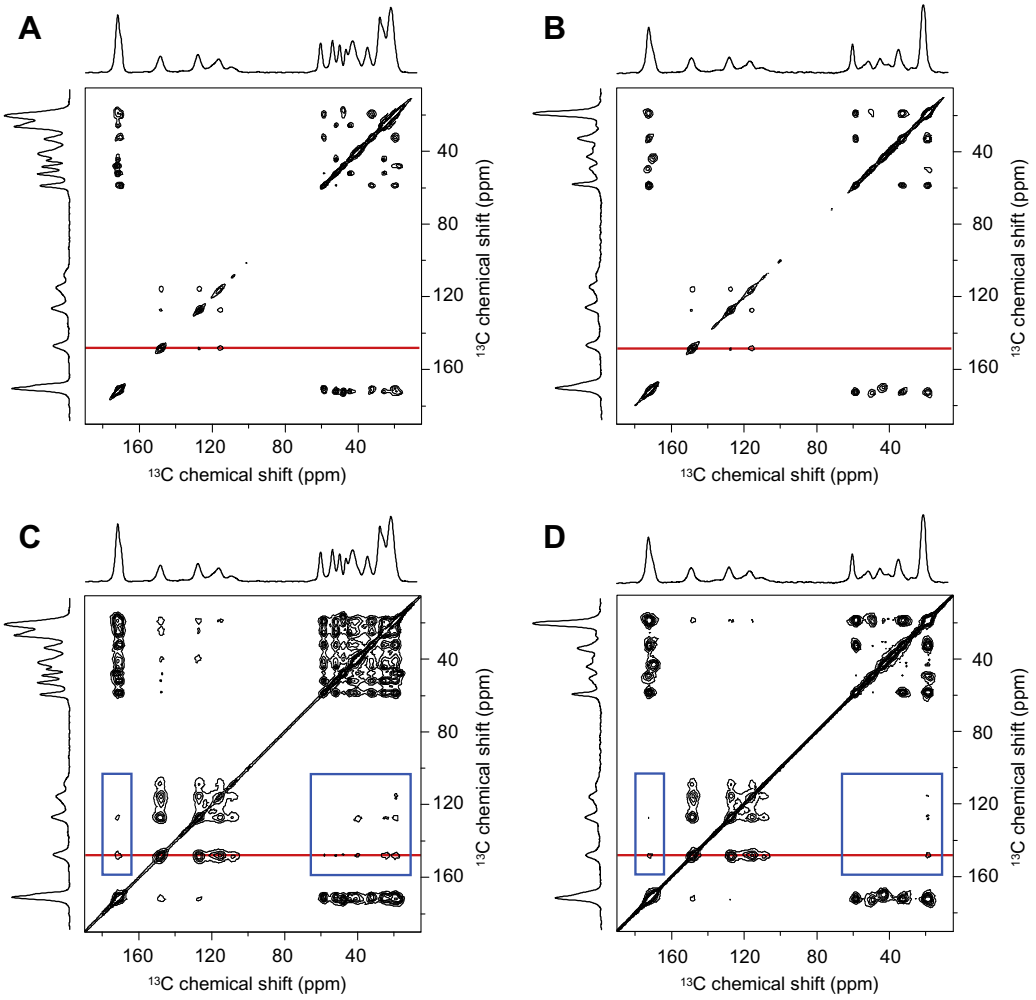

Figure 3. 2D covariance-processed DARR spectra at mixing times of 50 ms (**A** and **B**) and 500 ms (**C** and **D**). The samples are Aβ42 fibrils labeled at positions 17–21 mixed with curcumin labeled at the aromatic carbons (**A** and **C**), and Aβ42 fibrils labeled at the N-terminus mixed with curcumin labeled at the aromatic carbons (**B** and **D**). The number of acquisitions was 320 scans (**A** and **B**) and 400 scans (**C** and **D**) per increment. 1D cross-section spectra at the red lines are shown in Figure 4. Enlarged displays of the regions framed by the blue lines are shown in Figure 5.

On the other hand, in the covariance-processed 2D DARR spectrum of the N-terminus (Figs. 4D and 5B), only V12 of the Aβ42 fibrils appears to have a cross peak with curcumin. Although many researchers reported that the residues at positions 1–9 of the Aβ42 fibrils are unstructured, it is controversial whether the residues around positions 10–15 form a β-sheet.[16–23] These discrepancies might be due to differences in analytical methods or sample preparation conditions. To estimate the secondary structure at V12 of the Aβ42 fibrils in the present study, we evaluated the deviations of the ^{13}C chemical shifts relative to those of their corresponding random coil ($\Delta\delta = \delta_{observed} - \delta_{random\ coil}$). Wishart et al.[71,72] reported that the $\Delta\delta$ values of carbonyl carbons and $^{13}C_{\alpha}$ are positive in α-helices and negative in β-sheets and those of $^{13}C_{\beta}$ are negative in α-helices and positive in β-sheets. In our study (Table S1), the $\Delta\delta$ values of $^{13}C{=}O$ (−1.6) and $^{13}C_{\alpha}$ (−2.2) at V12 were negative and that of $^{13}C_{\beta}$ at V12 (+1.9) was positive; this suggests that V12 could form a β-sheet. Moreover, the line widths of ^{13}C in V12 were narrower than those of A2, F4, and G9 (Fig. 2B). The line widths and chemical shifts of ^{13}C in V12 without curcumin are almost the same as those with curcumin (Fig. 2, Fig. S4, and Table S1). Thus, curcumin would interact with V12 in the β-sheet conformation. On the other hand, the cross peaks of curcumin with A2, F4, and G9 of the Aβ42 fibrils are considerably weaker (Figs. 4D and 5B). The weaker cross peaks between curcumin and the N-terminus of the Aβ42 fibrils can be attributed to their weak interaction and/or the weak signal intensity of the carbons in the N-terminus, which results from broader line width and less efficient cross polarization for carbons in a random coil.

To investigate the effect of curcumin on the secondary structure of the Aβ42 fibrils, the ^{13}C-labeled Aβ42 fibrils without curcumin were prepared and analyzed by the 2D DARR experiments (Fig. S4). The assigned ^{13}C chemical shifts of the Aβ42 fibrils with and without curcumin are shown in Tables S1 and S2. Most of the chemical shift differences between the Aβ42 fibrils with and without curcumin were less than 0.2 ppm, indicating that the secondary structure of the Aβ42 fibrils did not significantly change after 1-h incubation with curcumin. This agrees with our TEM results showing that curcumin did not significantly change the fibril morphology within one hour (Fig. S2).

Note that the aromatic carbon atoms 7 (7') and/or 8 (8') of curcumin at 148.6 ppm had many clear cross peaks with the Aβ42 fibrils (Fig. 5). This indicates that methoxy and/or hydroxy groups adjacent to these aromatic carbons could be important for the interaction between curcumin and the Aβ42 fibrils. This agrees with the results of previous structure–activity studies suggesting that methylation of the phenolic hydroxy group in curcumin reduces its binding activity to the Aβ42 fibils.[49] The 3' and 4' hydroxy groups of the B ring in flavonoids are reportedly crucial for their anti-aggregating activity.[73] Therefore, the adjacent functional groups of the aromatic rings in polyphenols might be closely

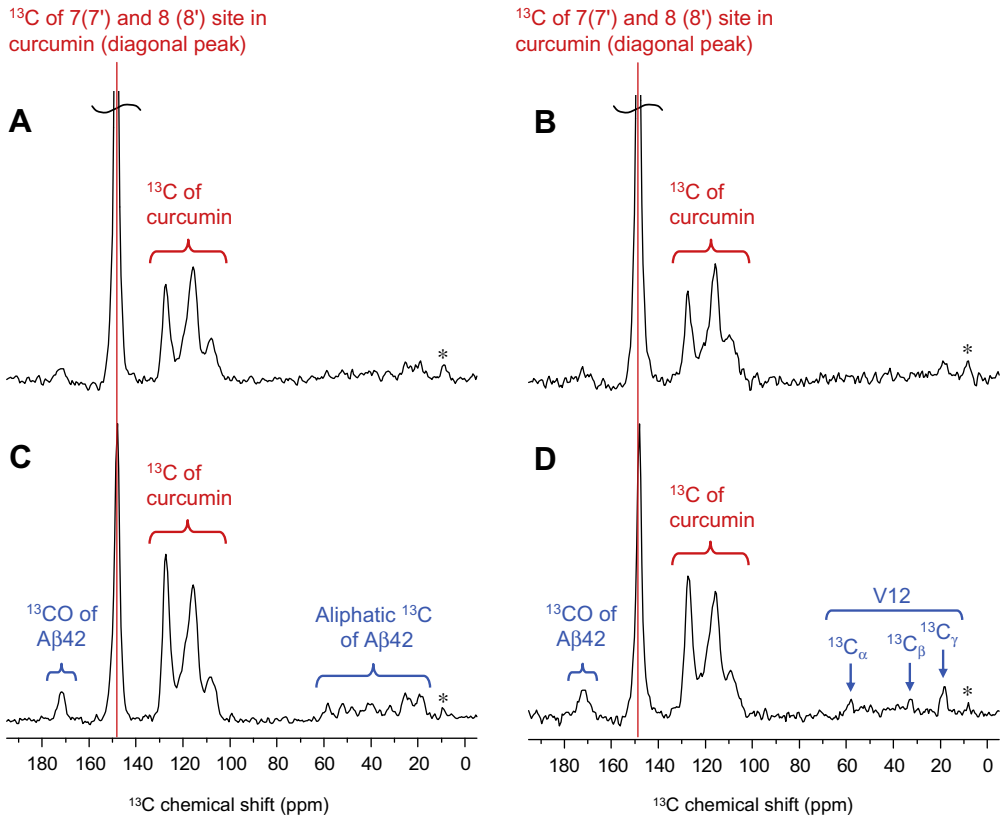

Figure 4. 1D cross-section spectra at ^{13}C chemical shift for positions 7(7') and 8 (8') of curcumin (δ 148.6 ppm, the red lines in Figure 3) of covariance-processed 2D DARR spectra. The samples are Aβ42 fibrils labeled at positions 17–21 mixed with curcumin labeled at the aromatic carbons for (**A**) and (**C**), and Aβ42 fibrils labeled at the N-terminus mixed with curcumin labeled at the aromatic carbons for (**B**) and (**D**). The mixing times were 50 ms for (**A**) and (**B**), and 500 ms for (**C**) and (**D**). The asterisked signal indicates the spinning side band of C7(7') and C8 (8') of curcumin.

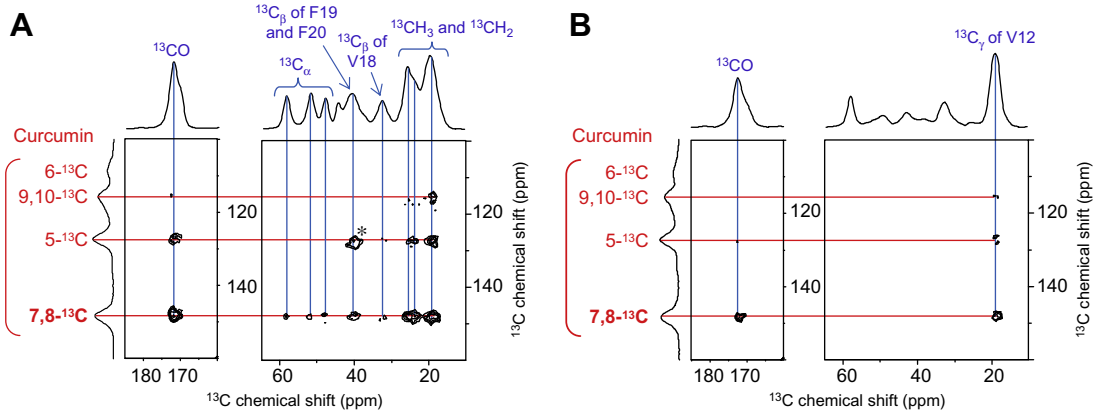

Figure 5. Enlarged displays of intermolecular cross peaks (the region framed by the blue line in Fig. 3C and D) in 2D covariance-processed DARR spectra at a mixing time of 500 ms. The samples are Aβ42 fibrils labeled at positions 17–21 mixed with curcumin labeled at the aromatic carbons (**A**), and Aβ42 fibrils labeled at the N-terminus mixed with curcumin labeled at the aromatic carbons (**B**). The asterisked cross peak might be due to intramolecular dipolar coupling between $^{13}C_β$ and naturally abundant aromatic ^{13}C in F19 and/or F20 of the Aβ42 fibrils.

related to the hydrophilic interactions with the Aβ42 fibrils. Since the aromatic carbon atom 5(5') at 127.9 ppm also possesses some clear cross peaks compared with carbons 9 (9') and/or 10 (10') (116.1 ppm) and carbon 6 (6') (109.1 ppm), this position might be also close to the Aβ42 fibrils, supporting the importance of the linker region between the aromatic rings of curcumin as previously reported.[49]

3. Conclusion

In this study, we analyzed the interaction sites of curcumin and the Aβ42 fibrils by solid-state NMR. Because the amount of bound curcumin was very small, it was difficult to analyze intermolecular dipole–dipole interactions between curcumin and the Aβ42 fibrils. However, we succeeded in detecting weak cross peaks between curcumin and the Aβ42 fibrils by using the covariance NMR method. The observed ^{13}C–^{13}C cross peaks suggested the binding of curcumin to 12th and 17–21st residues included in the β-sheet structure in the Aβ42 fibrils. Because the C-terminus of the Aβ42 fibrils also forms β-sheets, we expect that curcumin would also interact with the C-terminus. In fact, Sato and coworkers indicated that amyloid inhibitors could possibly interact with GxxxG motifs in the C-terminus of the Aβ fibrils.[74] The binding of curcumin to amyloid fibrils seems not to be site-specific like that of a ligand

to its receptor. We suppose curcumin would recognize repetitive structures of peptides and proteins which form intermolecular β-sheet. Since this 'semi-specific' binding of curcumin to amyloid fibrils is closely related to their clearance in vitro and in vivo, it is essential for analyzing binding mode of curcumin to the Aβ42 fibrils. We also suggested that the methoxy and/or hydroxy groups of curcumin play a significant role in its interaction with the Aβ42 fibrils. This information would be important for screening and development of aggregation inhibitors.

4. Material and methods

4.1. General

Following spectroscopic and analytical instruments were used: electron ionization mass spectrometry (EI–MS) and fast atom bombardment mass spectrometry (FAB-MS), JEOL JMS-600H (JEOL, Akishima, Japan); peptide synthesizer, Pioneer™ peptide synthesizer (Applied Biosystems, Foster City, CA); HPLC, Waters 600E multisolvent delivery system with a 2487 UV dual λ absorbance detector (Waters, Milford, MA); matrix-assisted laser desorption/ionization time-of-flight mass spectrometry (MALDI-TOF-MS), 4700 Proteomics Analyzer (Applied Biosystems); TEM, H-7650 (Hitachi High-Technologies, Ibaraki, Japan); solid-state NMR spectrometer, JEOL ECA-600 spectrometer and a custom-fabricated probe with a Chemagnetics 3.2 mm spinning system. HPLC was carried out on a Develosil packed column ODS-UG-5 (20 mm inner diameter × 150 mm) (Nomura Chemicals, Seto, Japan). Wakogel™ C-200 (silica gel, Wako Pure Chemical Industries, Osaka, Japan) was used for column chromatography.

HATU,[57] *N*-α-Fmoc amino acids, Fmoc-Ala-polyethylene glycol-polystyrene support (PEG-PS) resin, and *N,N*-diisopropylethylamine (DIPEA) were purchased from Applied Biosystems. *N,N*-Dimethylformamide (DMF), trifluoroacetic acid (TFA), 1,2-ethanedithiol, thioanisole, *m*-cresol, and diethyl ether (peroxide free) were purchased from Nacalai tesque (Kyoto, Japan). Piperidine was obtained from Sigma (St. Louis, MO). *N*-Fmoc-glycine ($^{13}C_2$,^{15}N) was purchased from Cambridge Isotope Laboratories (Andover, MD, USA). L-Alanine ($^{13}C_3$,^{15}N), L-phenylalanine (3-^{13}C), L-leucine ($^{13}C_6$,^{15}N), L-valine ($^{13}C_5$,^{15}N), and 4-hydroxy-3-methoxybenz-$^{13}C_6$-aldehyde (vanillin-$^{13}C_6$-ring) were purchased from Taiyo Nippon Sanso Corporation (Tokyo, Japan).

4.2. Preparation of protected amino acids labeled with ^{13}C and ^{15}N

Fmoc derivatives of L-alanine ($^{13}C_3$,^{15}N), L-leucine ($^{13}C_6$, ^{15}N), L-phenylalanine (3-^{13}C), and L-valine ($^{13}C_5$,^{15}N) were synthesized as previously reported.[75] The crude compounds were purified by column chromatography on Wakogel™ C-200 using hexane and increasing amounts of EtOAc containing 0.1% acetic acid, followed by recrystallization from hexane–EtOAc. The yields were 93–98%. Each structure was confirmed by ^1H NMR, ^{13}C NMR, and FAB-MS (matrix: glycerol) measurements.

4.3. Synthesis of Aβ derivatives labeled with ^{13}C and ^{15}N

The Aβ42 peptides labeled with stable isotopes (Fig. 1A and B) were synthesized in a stepwise manner on 0.1 mmol of preloaded Fmoc-Ala-PEG-PS resin by Pioneer™ using the Fmoc method as previously reported.[58] The coupling reaction was carried out using Fmoc amino acids (0.4 mmol), HATU (0.4 mmol), and DIPEA (0.8 mmol) in DMF for 30 min. After each coupling reaction, the N-terminal Fmoc group was removed with 20% piperidine in DMF.

After completing the chain elongation, each peptide resin was washed with DMF and dichloromethane and treated with a mixture containing TFA (16 mL), *m*-cresol (0.4 mL), thioanisole (2.4 mL), and ethanedithiol (1.2 mL) for final deprotection and cleavage from the resin. After shaking at room temperature for 2 h, the crude peptide was precipitated by diethyl ether and purified by RP-HPLC using the Develosil packed column (20 mm inner diameter × 150 mm) with elution at 8.0 mL/min by an 80 min linear gradient of 10–50% CH_3CN including 0.1% NH_4OH as previously reported.[59] Lyophilization gave the corresponding pure Aβ peptide, whose purity was confirmed by HPLC (>98%). Each purified peptide gave satisfactory mass spectral data on MALDI-TOF-MS (Fig. S5).

4.4. Synthesis of curcumin labeled at the aromatic carbons

The synthesis of ^{13}C-labeled curcumin (Fig. 1C) was based on the method developed by Pabon (Scheme S1).[60] Acetylacetone (0.03 mL, 0.300 mmol) and boric acid anhydride (14.4 mg, 0.207 mmol) were stirred for 0.5 h and formed a thick paste to which 0.13 mL of dry EtOAc was added. This mixture was then added to a solution of vanillin-$^{13}C_6$-ring (95.9 mg, 0.607 mmol) and 0.33 mL (281 mg) of tributylborate in 0.2 mL of dry EtOAc. After 10 min of stirring, *n*-butylamine (0.006 mL, 0.066 mmol) was added dropwise over a period of 10 min. The mixture was stirring for 4 h, followed by the addition of 0.5 mL of 0.6 N aqueous HCl at 60 °C and stirring was continued for 1 h to hydrolyze the reaction product. The organic layer was separated, and the aqueous layer was extracted three times with EtOAc. The combined EtOAc layer was washed with brine, dried over Na_2SO_4, and concentrated. The residue was purified by column chromatography on Wakogel™ C-200 using hexane and increasing amounts of EtOAc. Recrystallization from hexane–EtOAc gave the final product as orange needles with 45% yield. The structure was confirmed by ^1H and ^{13}C NMR (Figs. S6 and S7), and EI–MS measurements.

4.5. Preparation of aggregates (fibrils) of Aβ42 derivatives labeled with ^{13}C and ^{15}N mixed with curcumin labeled at the aromatic carbons

Each Aβ42 derivative was dissolved in 0.1% NH_4OH at 100 μM. After 10-fold dilution in 50 mM sodium phosphate containing 100 mM NaCl at pH 7.1, the resultant peptide solution (10 μM, pH 7.4) was incubated under quiescent conditions at 37 °C for 48 h. To the suspension, ^{13}C-labeled curcumin dissolved in EtOH was added. The final concentration of curcumin was 50 μM and that of EtOH was 2% (v/v). For comparison, the Aβ42 fibrils without curcumin (only EtOH was added so that the final concentration was 2%) were also prepared. The mixture was incubated for 1 h with gentle shaking every 10 min. After centrifugation at 17,712*g* and 4 °C followed by washing with distilled water, the resultant aggregates (fibrils) were dried in vacuo and used for solid-state NMR experiments. The weights of the samples used for the experiments were as follows: the Aβ42 fibrils labeled at positions 17–21 mixed with curcumin labeled at the aromatic carbons, 8.6 mg; the Aβ42 fibrils labeled at the N-terminus mixed with curcumin labeled at the aromatic carbons, 7.9 mg; the Aβ42 fibrils labeled at positions 17–21 without curcumin, 1.9 mg; the Aβ42 fibrils labeled at the N-terminus without curcumin, 1.6 mg.

4.6. TEM images of negatively stained preparations of Aβ42 fibrils and those mixed with curcumin

Fibrillation of Aβ42 was detected by a transmission electron microscope (Fig. S2). The incubation conditions were the same as those for preparing the samples for solid-state NMR. Each Aβ42 peptide was dissolved in 0.1% NH_4OH at 100 μM. After a 10-fold

dilution with 50 mM sodium phosphate containing 100 mM NaCl at pH 7.1, the resultant peptide solution (10 μM, pH 7.4) was incubated at 37 °C for 48 h. To the suspension, a solution of curcumin in EtOH or EtOH alone was added so that the final concentration of curcumin was 50 μM and that of EtOH was 2% (v/v). The mixture was incubated for 1 h with gentle shaking every 10 min. After centrifugation, the supernatant was removed from the pellets, and the aggregates were suspended in distilled water by gentle vortex mixing. The suspensions were applied to a 200-mesh Formvar-coated copper grid (Nissin EM, Tokyo, Japan) and dried in air before being negatively stained for a few seconds with 2% uranyl acetate. The aggregates were examined with the HITACHI H-7650 transmission electron microscope.

4.7. Solid-state NMR experiments

All solid-state NMR experiments in this study were performed at 14 T (600 MHz for ^{1}H) using a JEOL ECA-600 spectrometer and a custom-fabricated probe with a Chemagnetics 3.2 mm spinning system. The ^{13}C chemical shifts were calibrated in ppm relative to TMS by considering the ^{13}C chemical shift for methine ^{13}C of solid adamantane (29.5 ppm) as an external reference standard. All the experiments were carried out at a magic angle spinning (MAS) frequency of 21 kHz at room temperature. Increase in temperature due to sample spinning was estimated to be ca. 20°. We did not observe any change in chemical shifts and line widths of signals during our experiments, which proves a good thermal stability of our samples. For the broadband ^{13}C–^{13}C correlation 2D experiment, DARR[64,65] was used. Pulse sequence parameters of all NMR experiments were as follows: two pulse phase-modulated (TPPM) ^{1}H decoupling power = 80 kHz, RAMP-CP contact time = 1.7 ms, pulse delay = 2 s, t_1 increment = 23.7 μs, t_1 points of 2D = 144, and mixing time (τ_m) = 50 ms or 500 ms. A window function 'HAMMING' was used in all the 2D FT spectra to minimize t_1 noises.

4.8. Covariance processing of 2D DARR data

The 2D DARR data was zero-filled from 256 to 1024 points and processed by FT along the t_2 dimension. After phase correction, the resulting data matrix was used for covariance processing as previously reported.[50–53] We developed the calculation program. The covariance processing step was accelerated by singular value decomposition.[52]

Acknowledgments

We thank Dr. H. Fukuda at Theravalues Corporation for the MALDI-TOF-MS measurements. This work was partly supported by the Promotion of Science for Young Scientists (Grant No. 21.1128 to Y. M.) and Grant-in-aid for Scientific Research (A) (Grant No. 21248015 to K. I.) from the Ministry of Education, Culture, Sports, Science and Technology of the Japanese Government.

Supplementary data

Supplementary data (synthetic scheme for curcumin (Scheme S1), supplementary figures (Figs. S1–S7), supplementary tables (Tables S1, S2), and simulation study of the mixing time dependence of cross peak intensities in the 2D covariance-processed NMR spectra using two spin systems (Figs. S8–S10)) associated with this article can be found, in the online version, at doi:10.1016/j.bmc.2011.08.052.

References and notes

1. Selkoe, D. J. *Physiol. Rev.* **2001**, *81*, 741.
2. Glenner, G. G.; Wong, C. W. *Biochem. Biophys. Res. Commun.* **1984**, *120*, 885.
3. Masters, C. L.; Simms, G.; Weinman, N. A.; Multhaup, G.; McDonald, B. L.; Beyreuther, K. *Proc. Natl. Acad. Sci. U.S.A.* **1985**, *82*, 4245.
4. Kang, J.; Lemaire, H. G.; Unterbeck, A.; Salbaum, J. M.; Masters, C. L.; Grzeschik, K. H.; Multhaup, G.; Beyreuther, K.; Müller-Hill, B. *Nature* **1987**, *325*, 733.
5. Vetrivel, K. S.; Thinakaran, G. *Neurology* **2006**, *66*, S69.
6. Tickler, A. K.; Wade, J. D.; Separovic, F. *Protein Pept. Lett.* **2005**, *12*, 513.
7. Crouch, P. J.; Harding, S. M.; White, A. R.; Camakaris, J.; Bush, A. I.; Masters, C. L. *Int. J. Biochem. Cell Biol.* **2008**, *40*, 181.
8. Roher, A. E.; Lowenson, J. D.; Clarke, S.; Woods, A. S.; Cotter, R. J.; Gowing, E.; Ball, M. J. *Proc. Natl. Acad. Sci. U.S.A.* **1993**, *90*, 10836.
9. Jarrett, J. T.; Berger, E. P.; Lansbury, P. T., Jr. *Biochemistry* **1993**, *32*, 4693.
10. Davis-Salinas, J.; Saporito-Irwin, S. M.; Cotman, C. W.; Van Nostrand, W. E. *J. Neurochem.* **1995**, *65*, 931.
11. Malinchik, S. B.; Inouye, H.; Szumowski, K. E.; Kirschner, D. A. *Biophys. J.* **1998**, *74*, 537.
12. Serpell, L. C. *Biochim. Biophys. Acta* **2000**, *1502*, 16.
13. Tycko, R. *Biochemistry* **2003**, *42*, 3151.
14. Balbach, J. J.; Petkova, A. T.; Oyler, N. A.; Antzutkin, O. N.; Gordon, D. J.; Meredith, S. C.; Tycko, R. *Biophys. J.* **2002**, *83*, 1205.
15. Antzutkin, O. N.; Leapman, R. D.; Balbach, J. J.; Tycko, R. *Biochemistry* **2002**, *41*, 15436.
16. Williams, A. D.; Portelius, E.; Kheterpal, I.; Guo, J.; Cook, K. D.; Xu, Y.; Wetzel, R. *J. Mol. Biol.* **2004**, *335*, 833.
17. Whittemore, N. A.; Mishra, R.; Kheterpal, I.; Williams, A. D.; Wetzel, R.; Serpersu, E. H. *Biochemistry* **2005**, *44*, 4434.
18. Lührs, T.; Ritter, C.; Adrian, M.; Riek-Loher, D.; Bohrmann, B.; Döbeli, H.; Schubert, D.; Riek, R. *Proc. Natl. Acad. Sci. U.S.A.* **2005**, *102*, 17342.
19. Olofsson, A.; Sauer-Eriksson, A. E.; Ohman, A. *J. Biol. Chem.* **2006**, *281*, 477.
20. Olofsson, A.; Lindhagen-Persson, M.; Sauer-Eriksson, A. E.; Ohman, A. *Biochem. J.* **2007**, *404*, 63.
21. Tycko, R. Q. *Rev. Biophys.* **2006**, *39*, 1.
22. Paravastu, A. K.; Leapman, R. D.; Yau, W. M.; Tycko, R. *Proc. Natl. Acad. Sci. U.S.A.* **2008**, *105*, 18349.
23. Morimoto, A.; Irie, K.; Murakami, K.; Masuda, Y.; Ohigashi, H.; Nagao, M.; Fukuda, H.; Shimizu, T.; Shirasawa, T. *J. Biol. Chem.* **2004**, *279*, 52781.
24. Masuda, Y.; Irie, K.; Murakami, K.; Ohigashi, H.; Ohashi, R.; Takegoshi, K.; Shimizu, T.; Shirasawa, T. *Bioorg. Med. Chem.* **2005**, *13*, 6803.
25. Masuda, Y.; Uemura, S.; Nakanishi, A.; Ohashi, R.; Takegoshi, K.; Shimizu, T.; Shirasawa, T.; Irie, K. *Bioorg. Med. Chem. Lett.* **2008**, *18*, 3206.
26. Masuda, Y.; Uemura, S.; Ohashi, R.; Nakanishi, A.; Takegoshi, K.; Shimizu, T.; Shirasawa, T.; Irie, K. *ChemBioChem* **2009**, *10*, 287.
27. Masuda, Y.; Nakanishi, A.; Ohashi, R.; Takegoshi, K.; Shimizu, T.; Shirasawa, T.; Irie, K. *Biosci. Biotechnol. Biochem.* **2008**, *72*, 2170.
28. Selkoe, D. J. *Science* **2002**, *298*, 789.
29. Haass, C.; Selkoe, D. J. *Nat. Rev. Mol. Cell. Biol.* **2007**, *8*, 101.
30. Chimon, S.; Shaibat, M. A.; Jones, C. R.; Calero, D. C.; Aizezi, B.; Ishii, Y. *Nat. Struct. Mol. Biol.* **2007**, *14*, 1157.
31. Ahmed, M.; Davis, J.; Aucoin, D.; Sato, T.; Ahuja, S.; Aimoto, S.; Elliott, J. I.; Van Nostrand, W. E.; Smith, S. O. *Nat. Struct. Mol. Biol.* **2010**, *17*, 561.
32. Lorenzo, A.; Yankner, B. A. *Proc. Natl. Acad. Sci. U.S.A.* **1994**, *91*, 12243.
33. Soto, C.; Sigurdsson, E. M.; Morelli, L.; Kumar, R. A.; Castaño, E. M.; Frangione, B. *Nat. Med.* **1998**, *4*, 822.
34. Porat, Y.; Abramowitz, A.; Gazit, E. *Chem. Biol. Drug Des.* **2006**, *67*, 27.
35. Masuda, M.; Suzuki, N.; Taniguchi, S.; Oikawa, T.; Nonaka, T.; Iwatsubo, T.; Hisanaga, S.; Goedert, M.; Hasegawa, M. *Biochemistry* **2006**, *45*, 6085.
36. Feng, Y.; Wang, X. P.; Yang, S. G.; Wang, Y. J.; Zhang, X.; Du, X. T.; Sun, X. X.; Zhao, M.; Huang, L.; Liu, R. T. *Neurotoxicology* **2009**, *30*, 986.
37. Wang, J.; Ho, L.; Zhao, W.; Ono, K.; Rosensweig, C.; Chen, L.; Humala, N.; Teplow, D. B.; Pasinetti, G. M. *J. Neurosci.* **2008**, *28*, 6388.
38. Hamaguchi, T.; Ono, K.; Yamada, M. C. N. S. *Neurosci. Ther.* **2010**, *16*, 285.
39. Ganguli, M.; Chandra, V.; Kamboh, M. I.; Johnston, J. M.; Dodge, H. H.; Thelma, B. K.; Juyal, R. C.; Pandav, R.; Belle, S. H.; DeKosky, S. T. *Arch. Neurol.* **2000**, *57*, 824.
40. Ono, K.; Hasegawa, K.; Naiki, H.; Yamada, M. *J. Neurosci. Res.* **2004**, *75*, 742.
41. Yang, F.; Lim, G. P.; Begum, A. N.; Ubeda, O. J.; Simmons, M. R.; Ambegaokar, S. S.; Chen, P. P.; Kayed, R.; Glabe, C. G.; Frautschy, S. A.; Cole, G. M. *J. Biol. Chem.* **2005**, *280*, 5892.
42. Lim, G. P.; Chu, T.; Yang, F.; Beech, W.; Frautschy, S. A.; Cole, G. M. *J. Neurosci.* **2001**, *21*, 8370.
43. Garcia-Alloza, M.; Borrelli, L. A.; Rozkalne, A.; Hyman, B. T.; Bacskai, B. J. *J. Neurochem.* **2007**, *102*, 1095.
44. Begum, A. N.; Jones, M. R.; Lim, G. P.; Morihara, T.; Kim, P.; Heath, D. D.; Rock, C. L.; Pruitt, M. A.; Yang, F.; Hudspeth, B.; Hu, S.; Faull, K. F.; Teter, B.; Cole, G. M.; Frautschy, S. A. *J. Pharmacol. Exp. Ther.* **2008**, *326*, 196.
45. Baum, L.; Ng, A. *J. Alzheimer's Dis.* **2004**, *6*, 367.
46. Smith, D. G.; Cappai, R.; Barnham, K. J. *Biochim. Biophys. Acta* **2007**, *1768*, 1976.
47. Bandyopadhyay, S.; Huang, X.; Lahiri, D. K.; Rogers, J. T. *Expert Opin. Ther. Targets* **2010**, *14*, 1177.
48. Alavez, S.; Vantipalli, M. C.; Zucker, D. J.; Klang, I. M.; Lithgow, G. J. *Nature* **2011**, *472*, 226.
49. Reinke, A. A.; Gestwicki, J. E. *Chem. Biol. Drug Des.* **2007**, *70*, 206.
50. Brüschweiler, R.; Zhang, F. *J. Chem. Phys.* **2004**, *120*, 5253.
51. Brüschweiler, R. *J. Chem. Phys.* **2004**, *121*, 409.
52. Trbovic, N.; Smirnov, S.; Zhang, F.; Brüschweiler, R. *J. Magn. Reson.* **2004**, *171*, 277.

53. Hu, B.; Amoureux, J. P.; Trebosc, J.; Deschamps, M.; Tricot, G. *J. Chem. Phys.* **2008**, *128*, 134502.
54. Gazit, E. *FASEB J.* **2002**, *16*, 77.
55. Hexem, J. G.; Frey, M. H.; Opella, S. J. *J. Am. Chem. Soc.* **1981**, *103*, 224.
56. Naito, A.; Ganapathy, S.; McDowell, C. A. *J. Chem. Phys.* **1981**, *74*, 5393.
57. Carpino, L. A. *J. Am. Chem. Soc.* **1993**, *115*, 4397.
58. Irie, K.; Oie, K.; Nakahara, A.; Yanai, Y.; Ohigashi, H.; Wender, P. A.; Fukuda, H.; Konishi, H.; Kikkawa, U. *J. Am. Chem. Soc.* **1998**, *120*, 9159.
59. Murakami, K.; Irie, K.; Morimoto, A.; Ohigashi, H.; Shindo, M.; Nagao, M.; Shimizu, T.; Shirasawa, T. *Biochem. Biophys. Res. Commun.* **2002**, *294*, 5–10.
60. Pabon, H. J. J. *Recl. Trav. Chim. Pays-Bas* **1964**, *83*, 379.
61. Hudson, S. A.; Ecroyd, H.; Kee, T. W.; Carver, J. A. *FEBS J.* **2009**, *276*, 5960.
62. Durairajan, S. S.; Yuan, Q.; Xie, L.; Chan, W. S.; Kum, W. F.; Koo, I.; Liu, C.; Song, Y.; Huang, J. D.; Klein, W. L.; Li, M. *Neurochem. Int.* **2008**, *52*, 741.
63. Metz, G.; Wu, X.; Smith, S. O. *J. Magn. Reson. A* **1994**, *110*, 219.
64. Takegoshi, K.; Nakamura, S.; Terao, T. *Chem. Phys. Lett.* **2001**, *344*, 631.
65. Takegoshi, K.; Nakamura, S.; Terao, T. *J. Chem. Phys.* **2003**, *118*, 2325.
66. Morcombe, C. R.; Gaponenko, V.; Byrd, R. A.; Zilm, K. W. *J. Am. Chem. Soc.* **2004**, *126*, 7196.
67. Weingarth, M.; Tekely, P.; Brüschweiler, R.; Bodenhausen, G. *Chem. Commun.* **2010**, *46*, 952.
68. Weingarth, M.; Masuda, Y.; Takegoshi, K.; Bodenhausen, G.; Tekely, P. *J. Biomol. NMR* **2011**, *50*, 129.
69. Pandey, N.; Strider, J.; Nolan, W. C.; Yan, S. X.; Galvin, J. E. *Acta Neuropathol.* **2008**, *115*, 479.
70. Hafner-Bratkovic, I.; Gaspersic, J.; Smid, L. M.; Bresjanac, M.; Jerala, R. *J. Neurochem.* **2008**, *104*, 1553.
71. Wishart, D. S.; Sykes, B. D. *J. Biomol. NMR* **1994**, *4*, 171.
72. Wishart, D. S.; Bigam, C. G.; Holm, A.; Hodges, R. S.; Sykes, B. D. *J. Biomol. NMR* **1995**, *5*, 67.
73. Akaishi, T.; Morimoto, T.; Shibao, M.; Watanabe, S.; Sakai-Kato, K.; Utsunomiya-Tate, N.; Abe, K. *Neurosci. Lett.* **2008**, *444*, 280.
74. Sato, T.; Kienlen-Campard, P.; Ahmed, M.; Liu, W.; Li, H.; Elliott, J. I.; Aimoto, S.; Constantinescu, S. N.; Octave, J. N.; Smith, S. O. *Biochemistry* **2006**, *45*, 5503.
75. Fields, C. G.; Fields, G. B.; Noble, R. L.; Cross, T. A. *Int. J. Peptide Protein Res.* **1989**, *33*, 298.